arXiv:cond-mat/0310505v2 [cond-mat.soft] 2 Sep 2005

An Algorithm for RNA Pseudoknots

M. Pillsbury and J. A. Taylor
Department of Physics, University of California, Santa Barbara, CA 93106, USA

H. Orland
Service de Physique Théorique, CEA Saclay, 91191 Gif-sur-Yvette Cedex, France

A. Zee
Institute of Theoretical Physics, University of California, Santa Barbara, CA 93106, USA and
Department of Physics, University of California, Santa Barbara, CA 93106, USA

We further develop the large N formalism presented by some of us in earlier works in order to recursively calculate the partition function of a singly pseudoknotted RNA. We demonstrate that this calculation takes time proportional to the sixth power of the length of the RNA. The algorithm itself is presented in a self-contained form for the convenience of readers interested in implementing it.

I. INTRODUCTION

An RNA molecule is a heteropolymer, consisting of four types of nucleotides—uracil (U), adenine (A), guanine (G) and cytosine (C)—which are linked into a chain by phosphate bonds. The nucleotides then form saturating hydrogen bonds with one another, with A bonding to U and C bonding to G. These bonds cause the RNA to fold up into a stable, three dimensional structure. The structure is further stabilized by the stacking interactions, where runs of adjacent bonds twist into the familiar Watson-Crick helices.

The folding process is believed to be roughly hierarchical[5, 6], in that the primary (one-dimensional) structure, defined as the sequence of nucleotides, determines the secondary (two-dimensional) structure. If one visualizes the RNA as a circle, tying the first nucleotide to the last, and then represents hydrogen bonds as arcs within the circle, the secondary structure is the structure that can be drawn without bonds crossing one another[1, 3]. The secondary structure is largely unaffected by the formation of the (three-dimensional) tertiary structure, which includes, among other things, pseudoknots. Pseudoknots are precisely those structures which *do* contain bonds that would cross each other inside the disk. Algorithms that allow for the prediction of certain pseudoknots exist. For instance, [8] allows for any number of bonds on the outside of the disk, as long as they do not cross. Our algorithm allows for a different set of topologies, enumerated in [2].

We only consider a basic model of RNA, in which we only account for the energies associated with bond formation and neglect stacking interactions, loop entropies, and steric constraints. Modern RNA folding algorithms tend to be more complex, especially towards secondary structure[10, 11], but we opt for a simpler approach for the sake of clarity in this paper. As a result, the implementation we outline here is merely an illustration; it is not useful for predicting the structure of folded RNA.

Let $-U_{ij}$ be the change in energy of forming a hydrogen bond between the ith and jth bases, and let $V_{ij} = \exp(U_{ij}/T)$ be the Boltzmann factor at temperature T. Then one can write the partition function as a sum of terms of the form $V_{i_1 i_2} V_{i_3 i_4} \dots V_{i_{n-1} i_n}$. The i_ks in the above sum must be unique because a base is saturated by a single hydrogen bond. Our partition function is then

$$Z_{L1} = 1 + \sum_{i<j} V_{ij} + \sum_{i<j<k<l} V_{ij} V_{kl} + \dots + \frac{1}{N^2} \sum_{i<j<k<l} V_{ik} V_{jl} + \dots \quad (1)$$

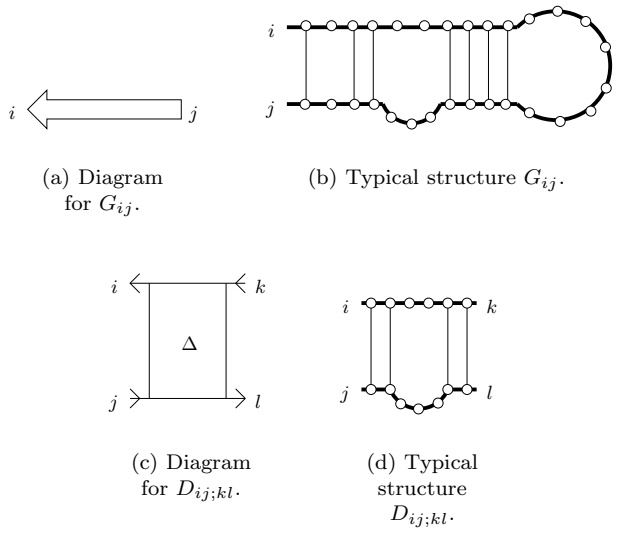
The factor of N is a parameter which tracks the topology of the bond structure. Since there is usually a small number of pseudoknots, and they can be controlled by the concentration of Mg^{++} ions in solution, we have introduced the parameter N, and penalize terms involving pseudoknots with factors of $1/N^2$. The secondary structure is $\mathcal{O}(1)$, while a restricted set of singly-pseudoknotted structures are $\mathcal{O}\left(N^{-2}\right)$[1].

There are many ($\sim L!$) possible terms in the above sum. We propose an algorithm which allows us to calculate this partition function to $\mathcal{O}\left(N^{-2}\right)$ in $\mathcal{O}\left(L^6\right)$ time. We also generalize this algorithm to calculate the partition function of an RNA that contains an arbitrary number of these $\mathcal{O}\left(N^{-2}\right)$ pseudoknots. We can then use backtracking to determine what bonds contribute to the dominant term in the partition function, and thus the folded structure at low temperatures. We can also determine the probability that a given bond is present at a finite temperature.

In order to express sums like (1) in a convenient fashion, we introduced two objects, which we call "propagators". The first of these is the two-indexed G_{ij}, which is the partition function of the secondary structure of a chain of nucleotides identical to that which lies between the jth base and the ith base. We set $G_{i,i+1} = 1$ and $G_{i,i+l} = 0$ for $l > 1$, which forbids "backwards propagation", insuring G_{ij} always runs in the $3'$ to $5'$ direction.

The other propagator is the four-indexed $\Delta_{ij;kl}$, which is non-zero if $i \geq k > l \geq j$. In that case, $\Delta_{ij;kl}$ is the partition function of the structure of two spatially separated, anti-parallel, chains of nucleotides, one between k and i, and the other between j and l, .

These definitions allow us to depict topological classes of structures with Feynman diagrams. In these diagrams, G_{ij} is an arrow pointing from j to i, and $\Delta_{ij;kl}$ is a box with solid sides with corners at i, j, k, and l. Individual V_{ij} bonds are dashed lines from i to j. These diagrams are typically in one-to-one correspondence with sums, as in [2]. The diagrams, as well as typical associated structures, are shown in fig. 1. In figs. 1(b) and 1(d), the heavy lines represent the RNA backbone, and the empty circles represent nucleotides.



(a) Diagram for G_{ij}.

(b) Typical structure G_{ij}.

(c) Diagram for $D_{ij;kl}$.

(d) Typical structure $D_{ij;kl}$.

FIG. 1: G and Δ.

We begin by summarizing the results relevant to a computer implementation of the algorithm are in section II. We present two variations on the algorithm. One allows for the calculation of the partition function with a single pseudoknot. The other allows for any number of pseudoknots. The remainder of the paper presents derivations of these results for the interested reader.

The index structure makes the topology of RNA folding similar to that of large N quantum chromodynamics, and these diagrams can be expressed using the t'Hooft double line formalism[4, 9]. We review the derivations of the recursive equations which define Δ and G, as well some other techniques and notations from [1] and [2], in section III.

Calculating the pseudoknot partition function is considerably more involved than backtracking the secondary structure partition function. Instead of a single, simple sum, many topologies must be summed over, and many of those involve summations over several indices. In order to do these sums efficiently, we define new propagators, similar to G and Δ, in section IV.

The procedure for calculating the partition function remains a recursive one, though. One finds the partition function $Z_{L+1,1}$ of an $L+1$ nucleotide RNA in terms of the structures of the L nucleotide RNA. This is simple enough for the secondary structure, because it is defined to exclude crossings. Thus, one considers only structures where a single bond arcs over complete secondary structures. This reasoning will lead one to the defining relation for G described in section III, and, indeed, it is how the equation was first derived[3].

However, crossings are the defining feature of pseudoknots, so our recursion relation will need to handle them. This requires the introduction of the "vertex operators" mentioned in section VI of [1]. These vertex operators are defined to be equal the partition functions of the secondary and pseudoknot structures on runs of nucleotides, with the additional requirement that a given nucleotide is unsaturated, so an incoming hydrogen bond can attach there. For example, the structure between the bases marked i and j in fig. 2 can be associated with a term in a vertex operator that allows an incoming bond from the $L+1$st base to connect at k.

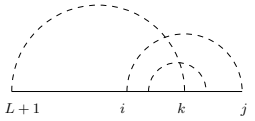


FIG. 2: The bond from $L+1$ to k is allowed when considering pseudoknots.

Once these vertex operators are put in a form similar to that of the pseudoknots in [2], which can be summed explicitly, it is possible to use them to write a recursion relation that can be used to generate a partition function that includes pseudoknots. Fortunately, the techniques needed to evaluate these vertex operators are very similar to those used to evaluate the pseudoknots. These calculations are described in section V.

II. ALGORITHM

Using the methods and results of the previous section, one can calculate the partition function of a singly pseudoknotted RNA with L nucleotides as follows:

1. Generate the matrix V_{ij} from the RNA sequence.

2. Solve the Hartree equation

$$G_{ij} = G_{i-1,j} + \sum_{k=j}^{i-1} V_{ik} G_{i-1,k+1} G_{k-1,j} + \delta_{i,j-1}$$

for G.

3. Use the result for G and the Bethe-Salpeter equa-

tion

$$D_{ij;kl} = V_{ij}\Bigg[\delta_{ik}\delta_{lj} + \sum_{m=k}^{i-1}\sum_{n=j+1}^{l} G_{i-1,m+1}D_{mn;kl}G_{n-1,j+1}\Bigg]$$

to find D.

4. Use D and G to determine E, K, and L.

$$E_{ij;kl} = \sum_{m=j}^{l}\sum_{n=k}^{i} D_{ij;nm}G_{n-1,k}G_{l,m+1}$$

$$K_{ij;kl} = \sum_{m=j}^{l}\sum_{n=k}^{i} D_{nj;km}G_{l,m+1}G_{i,n+1}$$

$$L_{ij;kl} = \sum_{m=j}^{l}\sum_{n=k}^{i} D_{im;nl}G_{n-1,k}G_{m-1,j}$$

5. Calculate the vertex Γ^J_{ij}, defined by

$$\Gamma^J_{ij} = E_{ij;J+1,J-1}$$

Then calculate the Θ^J_{ij}, defined by all the diagrams in fig. 10. The explicit sums associated with the terms in Θ^J_{ij} are contained in appendix A.

6. Use the recursion relation

$$\begin{aligned} Z_{L1} = {} & Z_{L-1,1} \\ & + \sum_{J=1}^{L-1} V_{LJ}\left(Z_{L-1,J+1}G_{J-1,1} + G_{L-1,J+1}Z_{L-1,1}\right) \\ & + \frac{1}{N}\sum_{J=1}^{L-1}\sum_{mn} V_{LJ}G_{L-1,m+1}\Gamma^J_{mn}G_{n-1,1} \\ & + \sum_{J=1}^{L-1}\sum_{mn} V_{LJ}G_{L-1,m+1}\Theta^J_{mn}G_{n-1,1} \end{aligned}$$

to find the partition function Z_{L1}.

Alternatively, one can find the partition function for an RNA with an arbitrary number of pseudoknots by replacing the recursion relation in step 5 with (39).

$$\begin{aligned} Z_{L1} &= Z_{L-1,1} \\ &+ \sum_{J=1}^{L-1} V_{LJ}Z_{L-1,J+1}Z_{J-1,1} \\ &+ \frac{1}{N}\sum_{J=1}^{L-1}\sum_{mn} V_{LJ}G_{L-1,m+1}\Gamma^J_{mn}G_{n-1,1} \\ &+ \sum_{J=1}^{L-1}\sum_{mn} V_{LJ}G_{L-1,m+1}\Theta^J_{mn}G_{n-1,1} \end{aligned}$$

We invite the interested reader to examine the derivation of the algorithm in the following sections. The algorithm can pick out knots. An example is shown in fig. 3, where the (one-pseudoknot) algorithm was applied to the sequence $AGUC$. The arcs represent hydrogen bonds.

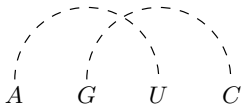


FIG. 3: Sample knot.

III. MATRIX FORMALISM AND STEEPEST DESCENT

In [1], two of the authors developed a formalism involving integrating over sets of matrices in order to exploit known results from quantum field theory. In this section, we review the techniques and notations associated with this formalism that we use in this article.

The analysis began with a demonstration that (1) is equivalent to

$$Z_{L1} = \frac{1}{N}\left.\frac{\partial}{\partial h}\right|_{h=0}\int dA\, e^{-\frac{N1}{2}\mathrm{tr}\,A^2}\left(\det M(A)\right)^N \qquad (2)$$

The integral is taken over the space of all $(L+1)\times(L+1)$ hermitian matrices A. $M(A)$ is a matrix function of A

$$M_{ij}(A) = \delta_{ij} - \delta_{i,j+1} + h\delta_{i1}\delta_{L+1,j} + i\sqrt{V_{i-1,j}}\,A_{i-1,j} \qquad (3)$$

In matrix form, this reads

$$M(A) = \begin{pmatrix} 1 & 0 & 0 & \dots & 0 & h \\ -1 & 1+a_{12} & a_{13} & \dots & a_{1L} & 0 \\ a^*_{12} & -1 & 1+a_{23} & \dots & a_{2L} & 0 \\ \vdots & \vdots & \vdots & \ddots & \vdots & \vdots \\ a^*_{1L} & a^*_{2L} & \dots & a^*_{L-1,L} & -1 & 1 \end{pmatrix} \qquad (4)$$

Here, we have abbreviated the notation so that

$$\begin{aligned} a_{ij} &= iV_{ij}^{\frac{1}{2}}A_{ij} \qquad \text{for } i<j \\ a^*_{ij} &= iV_{ij}^{\frac{1}{2}}A_{ij} \qquad \text{for } j>i \end{aligned} \qquad (5)$$

Note that we use $V_{ij}^{\frac{1}{2}}$ to refer to the square root of the (i,j)th element of V.

We use the well-known identity $\det M = e^{\mathrm{tr}\,\log M}$ and evaluate the derivative in (2) to get

$$Z_{L1} = \int dA\, e^{-\frac{N}{2}\mathrm{tr}\,A^2 + N\mathrm{tr}\,\log M(A)} M^{-1}(A)_{L+1,1} \qquad (6)$$

We can define an expectation value for the function $O(A)$ relative to an action $S(A) = \frac{1}{2}\mathrm{tr}\,A^2 - \mathrm{tr}\,\log M(A)$ as

$$\langle O\rangle = \int dA e^{-NS(A)}O(A) \qquad (7)$$

This allows us to write the partition function in a particularly compact form.

$$Z_{L1} = \left\langle M^{-1}_{L+1,1} \right\rangle \tag{8}$$

We can use the steepest descent approach outlined in section V of [1] in order to calculate the quantities in brackets to $\mathcal{O}\left(N^{-2}\right)$. We expand (8) in terms of a matrix fluctuation x, which is defined by

$$A_{ij} = \tilde{A}_{ij} + V_{ij}^{\frac{1}{2}} y_{ij}/N^{\frac{1}{2}} = \tilde{A}_{ij} + x_{ij}/N^{\frac{1}{2}} \tag{9}$$

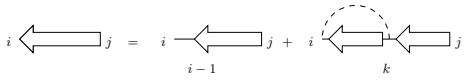
Here, $\tilde{A}_{ij}$ is stationary point of the action $S(A)$. We define

$$G_{ij} = M^{-1}(\tilde{A})_{i+1,j} \tag{10}$$

From this, it can be shown that the propagator G_{ij} satisfies a Hartree recursion relation.

$$G_{ij} = G_{i-1,j} + \sum_{k=j}^{i-1} V_{ik} G_{i-1,k+1} G_{k-1,j} + \delta_{i,j-1} \tag{11}$$

This can be solved after we impose boundary conditions. This equation is familiar from the RNA folding literature, and was first used in [3] to determine RNA secondary structure. This is to be expected, as G_{ij} is the secondary structure partition function for a run of nucleotides between j and i. Fig. 4 shows the defining relation for the Hartree propagator.



(a)

FIG. 4: Hartree equation for G_{ij}

Next, we find corrections to G_{ij} by expanding $S(\tilde{A} + x/\sqrt{N})$ as a power series in x. The first term in the action is just a quadratic,

$$\frac{1}{2}\mathrm{tr}\left(\tilde{A} + \frac{x}{N^{\frac{1}{2}}}\right)^2 = \frac{1}{2}\mathrm{tr}\,\tilde{A}^2 + \frac{1}{N^{\frac{1}{2}}}\mathrm{tr}\,\tilde{A}x + \frac{1}{2N}\mathrm{tr}\,x^2$$

Using the definitions in (3) and (10), we can write

$$\begin{aligned} M_{ij}\left(\tilde{A} + \frac{x}{N^{\frac{1}{2}}}\right) &= M_{ij}(\tilde{A}) + \frac{i}{\sqrt{N}} V^{\frac{1}{2}}_{i-1,j} x_{i-1,j} \\ &= \sum_{kl} M_{ik}(\tilde{A})\left(\delta_{kj} + \frac{i}{\sqrt{N}} M^{-1}_{kl}(\tilde{A}) V^{\frac{1}{2}}_{l-1,j} x_{l-1,j}\right) \\ \mathrm{tr}\,\log M\left(\tilde{A} + \frac{x}{N^{\frac{1}{2}}}\right) &= \mathrm{tr}\,\log M(\tilde{A}) + \mathrm{tr}\,\log\left(I + \frac{i}{\sqrt{N}} \sum_l G_{i-1,k} V^{\frac{1}{2}}_{k-1,j} x_{k-1,j}\right) \end{aligned}$$

If we define $R_{ij} = \sum_k G_{i-1,k} V^{\frac{1}{2}}_{k-1,j} x_{k-1,j}$, we can expand

$$\mathrm{tr}\,\log\left(I + i\frac{R}{N^{\frac{1}{2}}}\right) = \mathrm{tr}\,\left(i\frac{R}{N^{\frac{1}{2}}} + \frac{R^2}{N} + \dots\right)$$

Terms linear in x vanish because $\tilde{A}$ is the stationary point of $S(A)$, so our expectation value becomes

$$\langle O\rangle = C\int dx\,\exp\left[-\frac{1}{2}\left(\mathrm{tr}\,x^2 - \mathrm{tr}\,R^2\right) - \sum_{p=3}^{\infty}\frac{(-i)^p}{pN^{\frac{p}{2}-1}}\mathrm{tr}\,R^p\right] O \tag{12}$$

with the normalization C absorbing the Jacobian from the change of variables and various other constants (like $e^{-\frac{1}{2}\mathrm{tr}\,\tilde{A}^2}$).

We reintroduce the shorthand of [1] and [2] for powers and traces of powers of R in order to facilitate discussion of these expectation values.

$$B_p = R^p \tag{13}$$

$$T_p = \mathrm{tr}\,B_p \tag{14}$$

Now we can write

$$M^{-1}_{ij}\left(\tilde{A} + \frac{x}{N^{\frac{1}{2}}}\right) = \sum_k \left[\sum_{p=0}^{\infty}\frac{(-i)^p B_p}{N^{\frac{p}{2}}}\right]_{ik} G_{k-1,j} \tag{15}$$

using the power series for $(1+x)^{-1}$.

We call the free (i.e., quadratic) part of the action

$$S_0(x) = \frac{1}{2}\mathrm{tr}\,x^2 - \frac{1}{2}\mathrm{tr}\,R^2 \tag{16}$$

and use it to define the free expectation value,

$$\langle O\rangle_0 = \int dx e^{S_0(x)} O \tag{17}$$

The free action can be written in terms of a kernel Δ^{-1}, defined by

$$\begin{aligned} S_0(x) &= \sum_{i,j,k,l} x_{ij}\Delta^{-1}_{ij;kl}x_{kl} \\ \Delta^{-1}_{ij;kl} &= \delta_{il}\delta_{jk} - G_{l-1,i+1}G_{j-1,k+1}V_{ij}^{\frac{1}{2}}V_{kl}^{\frac{1}{2}} \end{aligned}$$

Multiplying the four-indexed Δ^{-1} by its inverse gives the Bethe-Salpeter relation

$$\begin{aligned} \Delta_{ij;kl} &= \delta_{ik}\delta_{lj} \\ &+ V_{ij}^{\frac{1}{2}}\sum_{m=k}^{i-1}\sum_{n=j+1}^{l} G_{i-1,m+1}V_{mn}^{\frac{1}{2}}\Delta_{mn;kl}G_{n-1,j+1} \end{aligned} \tag{18}$$

It is convenient to multiply this equation by $V_{ij}^{\frac{1}{2}}$ and $V_{kl}^{\frac{1}{2}}$ and define a slightly different propagator

$$D_{ij;kl} = V_{ij}^{\frac{1}{2}}\Delta_{ij;kl}V_{kl}^{\frac{1}{2}}$$

D obeys a new Bethe-Salpeter relation.

$$\begin{aligned} D_{ij;kl} = V_{ij}\Bigg[&\delta_{ik}\delta_{lj} \\ &+ \sum_{m=k}^{i-1}\sum_{n=j+1}^{l} G_{i-1,m+1}D_{mn;kl}G_{n-1,j+1}\Bigg] \end{aligned} \tag{19}$$

The diagrammatic form of this equation is shown in fig. III. We can use the D propagator to evaluate expectation values by Wick contracting xs, or we can do a coördinate transformation in our integral $x_{ij} = y_{ij}/V_{ij}^{\frac{1}{2}}$ and use D to contract ys, since the Jacobian associated with this change of variables is just a constant which can be absorbed into the normalization.

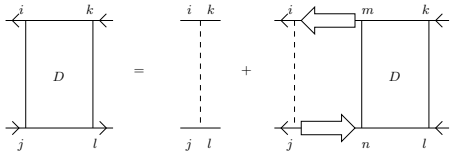


FIG. 5: Bethe-Salpeter equation for $D_{ij;kl}$

Solving (19) initially appears to be a task that will take $\mathcal{O}\left(L^6\right)$ time. However, the diagrammatic form of the equation indicates that $D_{ij;kl}$ can be written as

$$D_{i+1,j-1;k-1,l+1} = V_{i+1,j-1}V_{k-1,l+1}G_{ij;kl} \tag{20}$$

where the four-index G propagator $G_{ij;kl}$ is calculated in the same manner as G_{ij}, except the matrix V is modified so that $V_{mn} = 0$ if either $l > m > k$ or $l > n > k$. Calculating $G_{ij;kl}$ for a fixed k and l is then a $\mathcal{O}\left(L^3\right)$ task which much be performed $\mathcal{O}\left(L^2\right)$ times, meaning that D can be calculated in $\mathcal{O}\left(L^5\right)$ time.

Because G_{ij} represents the partition function of the possible secondary structures on the nucleotides between i and j inclusive, we should never see anything involving G that looks like a conventional matrix product, (e.g, $\sum_j G_{ij}D_{jk;mn}$), because that would include unphysical structures which have two hydrogen bonds ending at j. However, we see many terms of the form $\sum_j G_{ij}D_{j-1,k;mn}$, and so it is convenient, for an arbitrary matrix Q, to define a non-standard matrix product for sums involving G,

$$\begin{aligned} (QG)_{ij} &\equiv \sum_k Q_{ik}G_{k-1,j} \\ (GQ)_{ij} &\equiv \sum_k G_{i-1,k}Q_{kj} \end{aligned}$$

Using these definitions we can write a more explicit form of Z

$$\begin{aligned} Z_{L1} = \Bigg\langle &\exp\left[-\sum_{p=3}^{\infty}\frac{(-i)^p T_p}{pN^{\frac{p}{2}-1}}\right] \\ &\times\left[\left(\sum_{q=0}^{\infty}\frac{(-i)^q B_q}{N^{\frac{q}{2}}}\right)G\right]_{L+1,1}\Bigg\rangle_0 \end{aligned} \tag{21}$$

where we have used the series expansion for $M^{-1}(\tilde{A} + x/N^{\frac{1}{2}})$. This expression can then be expanded to $\mathcal{O}\left(N^{-2}\right)$, and the various terms can be evaluated using Wick's theorem.

IV. PROPAGATORS

The steepest descent expansion of (21) was completed in [2], and lead to a number of sums, each of which corresponds to a possible pseudoknot topology. While these sums need not be evaluated in order to calculate the partition function, many similar sums must be. As discussed in section I, each of these contributions will be expressed as sums involving D and G propagators, with indices running over appropriate ranges. In order to perform these summations efficiently, and describe them compactly, we must introduce new propagators. These are indexed objects similar to the already defined D and G, and they also fall into two classes, those which have two indices, and those which have four.

The first new two-indexed propagator is Z_{ij} itself, and the second, $\bar{Z}_{mn}$, is the pseudoknot contribution—that is, the $\mathcal{O}\left(N^{-2}\right)$ part of Z_{mn}. The different two-indexed propagators are related by the following equations,

$$Z_{ij} = G_{ij} + \frac{1}{N^2}\bar{Z}_{ij} \tag{22}$$

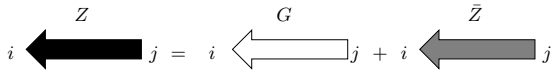


FIG. 6: Diagrams defining Z and $\bar{Z}$.

Now, one can see from the Bethe-Salpeter equation for $D_{ij;kl}$ that it always has bonds both between the ith and jth bases and between kth and lth bases. It is often convenient (and efficient) to make different assumptions about which bonds are implicitly defined when implementing a dynamic programming algorithm on a computer. To this end, we define new four-indexed propagators, the first of which is,

$$E_{ij;kl} = \sum_{p=k}^{i} \sum_{q=j}^{l} D_{ij;pq} G_{p-1,k} G_{l,q+1} \tag{23}$$

We draw $E_{ij;kl}$ in diagrams exactly like $D_{ij;kl}$, except that we draw it with a dotted edge between k and l to represent the fact that it doesn't contain an explicit hydrogen bond between those two nucleotides. The physical picture of the propagator $D_{ij;kl}$ presented in [2]—i.e., two spatially separated runs of nucleotides (one from j to l, the other from k to i) that form nucleotide bonds with each other—is equally applicable to E. However, instead of the two strands being bound to each other at both ends, here the inner ends of each strand may be loose.

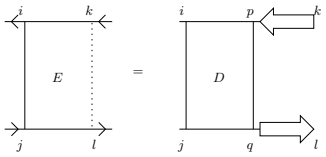


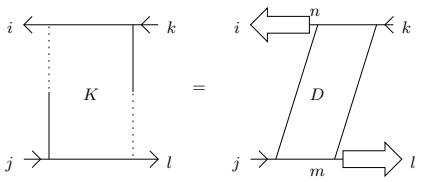
FIG. 7: Defining relation for $E_{ij;kl}$.

It's also useful to define two other four-indexed propagators, K and L. Both $K_{ij;kl}$ and $L_{ij;kl}$ have explicit bonds connecting i and j. However, $K_{ij;kl}$ is defined to have a bond connecting to k, but not necessarily to l. Likewise, $L_{ij;kl}$ will always have a bond connecting at l, but may not have a bond connecting to k.

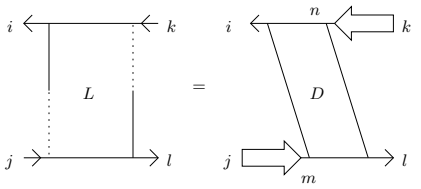
$$K_{ij;kl} = \sum_{m=j}^{l} \sum_{n=k}^{i} D_{nj;km} G_{l,m+1} G_{i,n+1} \tag{24}$$

$$L_{ij;kl} = \sum_{m=j}^{l} \sum_{n=k}^{i} D_{im;nl} G_{n-1,k} G_{m-1,j} \tag{25}$$

Diagrams for K and L have a dotted edge drawn to the nucleotide which doesn't have an explicit bond connecting to it, and solid edges drawn to the nucleotides that do attach to bonds.



(a) K



(b) L

FIG. 8: Diagrams for K and L.

Propagator	Explicitly bonded bases
$D_{ij;kl}$	i, j, k, and l
$E_{ij;kl}$	i and j
$K_{ij;kl}$	k and j
$L_{ij;kl}$	l and i

TABLE I: Four-indexed propagators

V. RECURSION RELATION AND VERTICES

In [1], two independent methods were presented that allowed one to calculate a partition function from (2), the integral over A. The first method was steepest descent, reviewed in section III, and which was carried to completion in [2]. The second method, involving recursively integrating out rows and columns of A, was presented in section VI of [1].

$$Z_{L1} = Z_{L-1,1} \tag{26}$$

$$+ \sum_{J=1}^{L-1} V_{LJ} \left\langle M^{-1}_{L,J+1}(x) \right\rangle \left\langle M^{-1}_{J,1}(x) \right\rangle \tag{27}$$

$$- \frac{1}{N} \sum_{J=1}^{L-1} V_{LJ} \left\langle M^{-1}_{L1}(x) M^{-1}_{J,J+1}(x) \right\rangle_C \tag{28}$$

$$+ \sum_{J=1}^{L-1} V_{LJ} \left\langle M^{-1}_{L,J+1}(x) M^{-1}_{J1}(x) \right\rangle_C \tag{29}$$

This method gives a recursion relation (to $\mathcal{O}\left(N^{-2}\right)$) for Z which depended on objects, called "vertices", which were not calculated explicitly. Here, we will use the steepest descent in order to find a form for the vertices that can be summed directly by a computer. It turns out that, in order to find a usable recursion relation, both methods must be used in concert.

In order to use (27) to find the $\mathcal{O}\left(N^{-2}\right)$ partition function, vertex operators for the insertion of bonds which cross other bonds are required. We can find these vertices by performing a steepest descent calculation on the *recursion relation* presented in section VI of [1], and then doing the fluctuation integral. This procedure will produce a modest proliferation of terms which can be interpreted with Feynman diagrams and then summed explicitly.

The first of these corrections, (27),

$$\sum_{J=1}^{L-1} V_{LJ} \left\langle M^{-1}_{L,J+1} \right\rangle \left\langle M^{-1}_{J,1} \right\rangle$$

is easy to evaluate because

$$\langle M^{-1}_{k+1,j}(x) \rangle = Z_{kj} \tag{30}$$

We need to truncate the product at $\mathcal{O}\left(N^{-2}\right)$. The result can be written in terms of the $\bar{Z}$ propagator introduced in (22).

$$\begin{aligned} \left\langle M^{-1}_{L,J+1} \right\rangle \langle M^{-1}_{J1} \rangle &= Z_{L-1,J+1} Z_{J-1,1} \\ &= G_{L-1,J+1} G_{J-1,1} + G_{L-1,J+1} \bar{Z}_{J-1,1} \\ &\quad + \bar{Z}_{L-1,J+1} G_{J-1,1} + \mathcal{O}\left(N^{-4}\right) \end{aligned} \tag{31}$$

Next we calculate (28) by doing the fluctuation integral $\left\langle M^{-1}_{L1} M^{-1}_{J,J+1} \right\rangle$ by Wick contraction, as detailed in appendix B. This yields

$$\left\langle M^{-1}_{L1} M^{-1}_{J,J+1} \right\rangle_C = -\sum_{i,\ldots,l} G_{L-1,i+1} G_{j-1,1} D_{ij;kl} G_{k-1,J+1} G_{J-1,l+1} = -\sum_{ij} G_{L-1,i+1} \Gamma^J_{ij} G_{j-1,1} \tag{32}$$

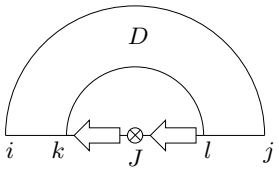


FIG. 9: Diagram of Γ^J_{ij}

Here, we have introduced the amputated vertex operator Γ, which can be defined very simply in terms of E.

$$\Gamma^J_{ij} = E_{ij;J+1,J-1} \tag{33}$$

The remaining term in the recursion relation is

$$\left\langle M^{-1}_{L,J+1} M^{-1}_{J1} \right\rangle_C = \left\langle \exp\left(-\sum_{p=3}^{\infty} \frac{(-i)^p T_p}{p N^{p/2-1}} \right) \left[\left(\sum_{q=0}^{\infty} \frac{(-i)^q B_q}{N^{q/2}} \right) G \right]_{L,J+1} \left[\left(\sum_{r=0}^{\infty} \frac{(-i)^r B_r}{N^{r/2}} \right) G \right]_{J1} \right\rangle_{0,C}$$

This expands out to

$$\begin{aligned} \frac{1}{N^2} \Big\langle & (B_1 G)(B_3 G) + (B_2 G)(B_2 G) + (B_3 G)(B_1 G) \\ & + \frac{T_3}{3} \left[(B_1 G)(B_2 G) + (B_2 G)(B_1 G) \right] \\ & + \left[\frac{T_4}{4} + \frac{T_3^2}{9} \right] (B_1 G)(B_1 G) \Big\rangle_{0,C} \end{aligned} \tag{34}$$

We suppres the indices on these terms because they are all the same: $(B_p G)_{L,J+1} (B_q G)_{J-1,1}$. These can be evaluated the same way that the terms in (32) were, by Wick contracting the powers of x implicit in the Ts and Bs. This is detailed in appendix B. Diagrams representing each term are shown in fig. 10, and explicit summations are contained in appendix A.

These are modifications of diagrams calculated in [2], with an unsaturated nucleotide than can accept a hydrogen bond at J. Not all diagrams in [2] are modified this way, nor are all insertion points included, because doing so would produce pseudoknots of $\mathcal{O}\left(N^{-4}\right)$. We have further simplified notation by suppressing the Gs and angle brackets. It is also convenient to discuss "amputated" vertices, that is, the sum of all the terms in (34) and (32) with the external $G_{L-1,i}$ and $G_{j-1,1}$ propagators removed. This amputation insures that there are bonds attaching to the subscript indices of both Θ^J_{ij} and Γ^J_{ij}.

$$Z_{L1} = Z_{L-1,1} \tag{35}$$
$$+ \sum_{J=1}^{L-1} V_{LJ} \left(Z_{L-1,J+1} G_{J-1,1} + G_{L-1,J+1} Z_{L-1,1} \right) \tag{36}$$
$$+ \frac{1}{N} \sum_{J=1}^{L-1} \sum_{mn} V_{LJ} G_{L-1,m+1} \Gamma^J_{mn} G_{n-1,1} \tag{37}$$
$$+ \sum_{J=1}^{L-1} \sum_{mn} V_{LJ} G_{L-1,m+1} \Theta^J_{mn} G_{n-1,1} \tag{38}$$

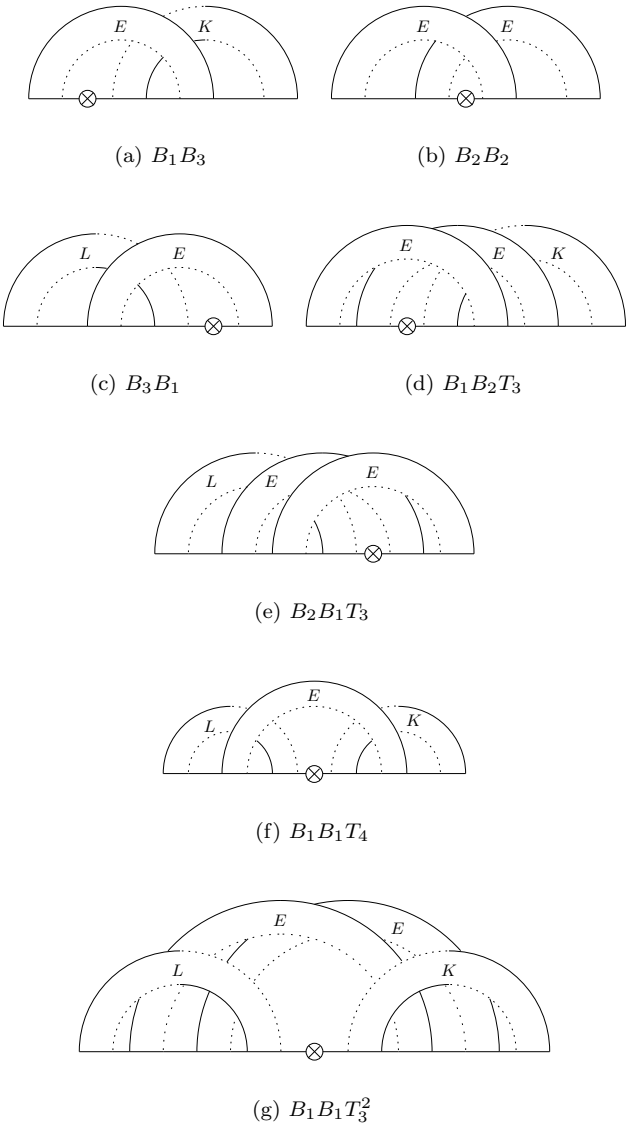
Using the definitions for the vertex operators Γ^J_{ij} and Θ^J_{ij}, as well as the relation (35), we can recursively calculate the partition function for an RNA that contains a single pseudoknot. However, we can easily extend this equation so that it consistently accounts for RNAs that have any number of pseudoknots. This is done by "filling in" the G propagators in (35) terms of the relation, to turn them into Zs with no penalty to efficiency.

$$Z_{L1} = Z_{L-1,1} \tag{39}$$
$$+ \sum_{J=1}^{L-1} V_{LJ} Z_{L-1,J+1} Z_{J-1,1} \tag{40}$$
$$+ \frac{1}{N} \sum_{J=1}^{L-1} \sum_{mn} V_{LJ} G_{L-1,m+1} \Gamma^J_{mn} G_{n-1,1} \tag{41}$$
$$+ \sum_{J=1}^{L-1} \sum_{mn} V_{LJ} G_{L-1,m+1} \Theta^J_{mn} G_{n-1,1} \tag{42}$$

VI. CONCLUSION

It may be apparent that the execution time of the algorithm presented here grows as L^6, because the limiting step is the calculation of the various vertices. Though a few of them actually require more than the three indices and three summations implied by that order, those sums can be restricted in a manner similar to that used to calculate the four-indexed propagators.

The model for bonding we use is somewhat simplistic, in that we account only for independent bonds. However, it should not be difficult to incorporate stacking interactions, or loop penalties, or other more advanced scoring methods into the algorithm, while retaining the topologies and recursion relation obtained from the large N analysis.



(a) B_1B_3 (b) B_2B_2 (c) B_3B_1 (d) $B_1B_2T_3$ (e) $B_2B_1T_3$ (f) $B_1B_1T_4$ (g) $B_1B_1T_3^2$

FIG. 10: Distinct terms in Θ^J_{ij}

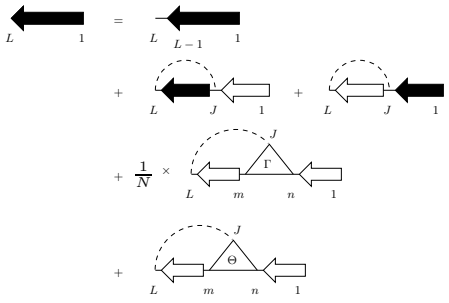


FIG. 11: Diagram form of recursion.

APPENDIX A: EXPLICIT VERTICES

The $\mathcal{O}(N^{-2})$ vertex term, Θ_{ij}^{J} is, as shown in section V, a sum of several terms. While these terms are shown in diagrammatic form in fig. 10, we also present the explicit summations in this appendix, to simplify efforts to implement the algorithm.

$$\langle B_1 B_3 \rangle_0 = \sum_{l=j}^{J-2} \sum_{k=l+1}^{J-1} E_{i,l+1;J+1,k-1} K_{J-1,j;kl} \tag{A1}$$

$$\langle B_2 B_2 \rangle_0 = \sum_{l=j}^{J-2} \sum_{k=J+2}^{i} E_{i,l+1;k,J-1} E_{k-1,j;J+1,l} \tag{A2}$$

$$\langle B_3 B_1 \rangle_0 = \sum_{l=J+1}^{i-1} \sum_{k=l+1}^{i} L_{i,J+1;kl} E_{k-1,j;l+1,J-1} \tag{A3}$$

$$\langle B_1 B_2 T_3 \rangle_0 = \sum_{l=j}^{J-3} \sum_{n=l+1}^{J-2} \sum_{m=n+1}^{J-1} \sum_{k=J+1}^{i} E_{i,n+1;k,m-1} E_{k-1,l+1;J+1,n} K_{J-1,j;ml} \tag{A4}$$

$$\langle B_2 B_1 T_3 \rangle_0 = \sum_{l=j}^{J-2} \sum_{n=J+2}^{i-2} \sum_{m=n+1}^{i-1} \sum_{k=m+1}^{i} L_{i,J+1,k,n-1} E_{k-1,l+1;m,J-1} E_{m-1,j;nl} \tag{A5}$$

$$\langle B_1 B_1 T_4 \rangle_0 = \sum_{l=j}^{J-3} \sum_{n=l+1}^{J-2} \sum_{m=J+2}^{i-1} \sum_{k=m+1}^{i} L_{i,J+1;k,m-1} E_{k-1,l+1;mn} K_{J-1,j;n+1,l} \tag{A6}$$

$$\begin{aligned} \left\langle B_1 B_1 T_3^2 \right\rangle = & \sum_{l=j}^{J-4} \sum_{n=l+1}^{J-3} \sum_{p=n+1}^{J-2} \sum_{o=J+2}^{i-2} \sum_{m=o+1}^{i-1} \sum_{k=m+1}^{i} L_{i,J+1;k,o-1} E_{k-1,n+1;mp} \\ & \times E_{m-1,l+1;on} K_{J-1,j;p+1,l} \end{aligned} \tag{A7}$$

APPENDIX B: EVALUATION OF INTEGRALS

We calculate (28) by evaluating the integral

$$\left\langle M_{L1}^{-1} M_{J,J+1}^{-1} \right\rangle_C = \left\langle \exp\left(-\sum_{p=3}^{\infty} \frac{(-i)^p}{p N^{p/2-1}} T^p \right) \left[\left(\sum_{q=0}^{\infty} \frac{(-i)^q}{N^{q/2}} B_q \right) G \right]_{L1} \left[\left(\sum_{r=0}^{\infty} \frac{(-i)^r}{N^{r/2}} B_r \right) G \right]_{J,J+1} \right\rangle_{0,C} \tag{B1}$$

$$= \left\langle \left(1 - \frac{i\,T_3}{3N^{\frac{1}{2}}} - \frac{T_4}{4N} - \frac{T_3^2}{18N} \right) \left[\left(1 - \frac{i\,B_1}{N^{1/2}} - \frac{B_2}{N} \right) G \right]_{L1} \left[\left(1 - \frac{i\,B_1}{N^{\frac{1}{2}}} - \frac{B_2}{N} \right) G \right]_{J,J+1} \right\rangle_{0,C} \tag{B2}$$

We have only expanded to $\mathcal{O}\left(N^{-1}\right)$ because of the explicit factor of $1/N$ in (28). The $\mathcal{O}\left(N^{-\frac{1}{2}}\right)$ terms vanish by symmetry, since they depend on odd powers of x, so this simplifies to

$$\left\langle M_{L1}^{-1} M_{J,J+1}^{-1} \right\rangle_C = \left\langle G_{L1} G_{J,J+1} \left[1 - \frac{1}{N} \left(\frac{T_4}{4} + \frac{T_3^2}{18} \right) \right] - \frac{T_3}{3N} \left[(B_1 G)_{L1} G_{J,J+1} + G_{L1} (B_1 G)_{J,J+1} \right] \right.$$
$$\left. - \frac{1}{N} \left[(B_2 G)_{L1} G_{J,J+1} + G_{L1} (B_2 G)_{J,J+1} \right] - \frac{1}{N} (B_1 G)_{L1} (B_1 G)_{J,J+1} \right\rangle_{0,C} \tag{B3}$$

The $\mathcal{O}(1)$ term $\langle G_{L-1,1} G_{J-1,J+1} \rangle$ vanishes because it depends on the "backwards propagator" $G_{J-1,J+1}$. Four $\mathcal{O}\left(N^{-1}\right)$ terms, $\langle T_4 G_{L-1,1} G_{J-1,J+1} \rangle$, $\left\langle T_3^2 G_{L-1,1} G_{J-1,J+1} \right\rangle$, $\langle T_3 (B_1 G)_{L1} G_{J-1,J+1} \rangle$ and $\langle (B_2 G)_{L1} G_{J-1,J+1} \rangle$, vanish for the same reason. This leaves us with only three terms to compute, $\langle T_3 G_{L-1,1} (B_1 G)_{J,J+1} \rangle$, $\langle G_{L-1,1} (B_2 G)_{J,J+1} \rangle$ and $\langle (B_1 G)_{L1} (B_1 G)_{J,J+1} \rangle$. The first two are shown in diagram form in figs. 13(a) and 13(b) respectively; they obviously vanish. The third is shown as a diagram in fig. 9 and can be written as an explicit sum,

$$\langle (B_1 G)_{L1} (B_1 G)_{J,J+1} \rangle_0 = \sum_{i,\ldots,l} G_{L-1,i+1} G_{j-1,1} D_{ij;kl} G_{k-1,J+1} G_{J-1,l+1} = \sum_{ij} G_{L-1,i+1} E_{ij;J+1,J-1} G_{j-1,1} \tag{B4}$$

The left hand side depends on L while the right hand side depends on $L-1$ because of the non-standard definition of matrix products that we introduced in section III.

The same integration technique applies to (34).

$$\left\langle M_{L,J+1}^{-1} M_{J1}^{-1} \right\rangle_C = \left\langle \left(1 - \frac{i\, T_3}{3N^{1/2}} - \frac{T_4}{4N} - \frac{T_3^2}{18N} \right) \right.$$
$$\left. \times \left[\left(1 - \frac{i\, B_1}{N^{1/2}} - \frac{B_2}{N} + \frac{i\, B_3}{N^{3/2}} \right) G \right]_{L,J+1} \left[\left(1 - \frac{i\, B_1}{N^{1/2}} - \frac{B_2}{N} + \frac{i\, B_3}{N^{3/2}} \right) G \right]_{J1} \right\rangle_{0,C} \tag{B5}$$

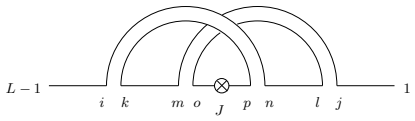
We drop some terms in the expansion because they cannot yield non-vanishing connected expectation values. The remaining terms can be expanded to $\mathcal{O}\left(N^{-2}\right)$. The fractional coefficients cancel over-counting in terms that depend on traces, which are symmetric under cyclic permutations of the xs.

As an example, we evaluate the first of the terms by Wick contraction. The contractions which remain are

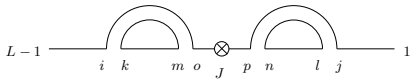
$$\langle (B_2 G)_{L,J+1} (B_2 G)_{J,1} \rangle_{0,C} = \sum_{i,\ldots,p} G_{L-1,i+1} G_{k-1,m+1} G_{o-1,J+1} G_{J-1,p+1} G_{n-1,l+1} G_{j-1,1} (D_{in;kp} D_{mj;ol} + D_{io;km} D_{pj;nl})$$
$$= \sum_{i,\ldots,l} G_{L,i+1} G_{j-1,1} E_{il;k+1,J-1} E_{kj;J+1,l-1} \tag{B6}$$

The first of the two Wick contractions is shown as a diagram in fig. 12(a), while the second term, shown in fig. 12(b), vanishes. The non-vanishing part can be greatly simplified with the use of the appropriate propagators. The advantage of the propagators introduced in section IV should now be obvious; we have reduced the number

of summed indices from eight to four.

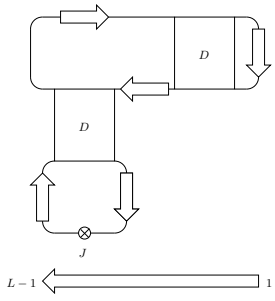


(a) Non-vanishing contraction

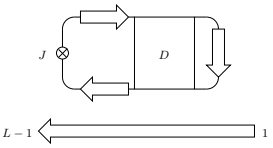


(b) Vanishing contraction.

FIG. 12: Contractions in $\langle B_2 B_2 \rangle$



(a) $\langle T_3 B_1 \rangle$



(b) $\langle B_2 \rangle$

FIG. 13: Vanishing contractions in Γ

[1] H. Orland and A. Zee, "RNA Folding and Large N Matrix Theory", \protect\vrule width0pt\protect\href{http://arxiv.org/abs/cond-mat/0106359}{cond-mat/0106359}.

[2] M. Pillsbury, H. Orland and A. Zee, "A steepest descent calculation of RNA", \protect\vrule width0pt\protect\href{http://arxiv.org/abs/physics/0207110}{physics/0207110}.

[3] R. Nussinov and A.B. Jacobson, PNAS **77** (1980) 6309.

[4] S. Coleman, *Aspects of Symmetry* (Cambridge University Press, New York, 1985), Ch. 9.

[5] P.G. Higgs, Quarterly Reviews in Biophysics **33** (2000) 199.

[6] I. Tinoco Jr. and C. Bustamante, J. Mol. Biol. **293** (1999) 271.

[7] M.S. Waterman and T.F. Smith, Adv. Applied Maths. **7** (1986)

[8] E. Rivas and S.R. Eddy, J. Mol. Biol. **285** (1999) 2053.

[9] G. 't Hooft, Nucl. Phys. B **72** (1974) 461.

[10] M. Zuker, Science **244** (1989) 48.

[11] J.A. Jaeger, D.H. Turner and M. Zuker, Proc. Nat. Acad. Sci. **86** (1989) 7706.

[12] D.K. Lubensky and D.R. Nelson, Phys. Rev. Lett. **85** (2000) 1572.

[13] I.L. Hofacker, W. Fontana, P.F. Stadler, L.S. Bonhoeffer, M. Tacker and P. Schuster, Monatshefte für Chemie **125** (1994) 167.

[14] A. Montanari and M. Mézard, Phys. Rev. Lett. **86** (2001) 2178.

[15] R. Bundschuh and T. Hwa, Phys. Rev. Lett. **83** (1999) 1479.

[16] J.S. McCaskill, Biopolymers 29 (1990) 1105.

[17] H. Zhou, Y. Zhang and Z-C. Ou-Yang, Phys. Rev. Lett. **86** (2001) 356.